AIChE

Mass Transport and Thermodynamic Analysis of PAHs in Partitioning Systems in the Presence and Absence of Ultrasonication

Pedro A. Isaza, Andrew J. Daugulis, and Kunal Karan
Dept. of Chemical Engineering, Queen's University, Kingston, ON, Canada K7L 3N6

DOI 10.1002/aic.12168
Published online January 27, 2010 in Wiley Online Library (wileyonlinelibrary.com).

Transport of PAHs from Desmopan polymers to methanol under various mixing conditions and in the presence of ultrasound was analyzed. PAH transport was influenced by external transport resistances; however, agitation greater than 800 rpm yielded PAH transport completely limited by internal resistances. Delivery rates of phenanthrene, fluoranthene, and pyrene with ultrasonication were faster than that under any mixing condition, suggesting enhanced internal transport properties. Ultrasound also induced increased concentrations of PAHs in solution at equilibrium. The model developed described PAH delivery under sonicated/non-sonicated conditions, while quantifying diffusive and thermodynamic properties. Diffusivities with and without ultrasound decreased with permeant molecular size agreeing with coefficients determined for similar aromatic compounds in polymers. Partitioning coefficients under sonicated and non-sonicated conditions conclusively differed from each other and decreased as a function of PAH molecular size. Quantitative structure-property relationship data of PAHs yielded factors predicting thermodynamic and transport behaviors, with polarizability being the best descriptor. © 2010 American Institute of Chemical Engineers *AIChE J,* 56: 2717–2726, 2010
Keywords: ultrasound, mass transfer, equilibrium, solid–liquid partitioning systems, PAHs

Introduction

Polycyclic aromatic hydrocarbons (PAHs) are comprised of two or more benzene rings fused in a linear, angular, or cluster arrangement and are naturally present at low levels in the environment. Industrial processes have resulted in an increased presence through the burning of gas, oil, coal, wood, garbage, and other organic substances.[1] The need to remove PAHs from the environment is driven by their carcinogenic nature, which imposes a human health risk in populated areas. Studies have shown that although lower molecular weight PAHs are not acutely toxic, increasing molecular size correlates well with carcinogenicity, environmental persistence, and chronic toxicity.[1–3] Currently, 16 PAHs are present in the US Environmental Protection Agency priority pollutant list.[2]

The removal and destruction of PAHs has been studied through numerous technologies.[4–7] Two-phase partitioning bioreactors (TPPBs) are a technology platform recently explored for biological degradation of PAHs.[8–16] In TPPB setups, an aqueous phase containing degrading micro-organisms co-exists with an immiscible second phase acting as a reservoir for high concentrations of hydrophobic pollutants.[17] Low levels of contaminants are then transported and partitioned into the aqueous phase, where microbes degrade these toxic substrates. TPPB fundamental principles of operation are governed by mass transport, thermodynamic, and biological considerations.

A recent study demonstrated that the sequestering phase of TPPBs was not restricted to immiscible organic solvents but could consist of solid polymeric compounds.[18] This provided an opportunity for the removal of hydrophobic

Correspondence concerning this article should be addressed to A. J. Daugulis at andrew.daugulis@chee.queensu.ca.

contaminants directly from soil, water, and air, as polymers have the ability to sorb organic compounds without inducing further environmental contamination. Once loaded, the polymers can then be introduced into a TPPB where pollutants would be microbially degraded. Such a remediation strategy was proposed and demonstrated for treating PAH contaminated soil.[15]

An important aspect of these solid–liquid bioreactors is inter-phase mass transfer, which has been demonstrated to restrict rates of degradation in these novel reactors for poorly water soluble substrates.[15] As noted, microbial uptake in TPPBs requires transport and partitioning of organic substrates into the aqueous phase before degradation.[19] Since polymer-aqueous systems introduce fixed interfacial areas for transport, it is not surprising that they may be subject to delivery limitations. Such constraints have been demonstrated for biphenyl as well as for PAHs.[15,20]

Potential solutions are present in the field of responsive drug delivery, which uses a variety of external stimuli to improve transport within and from polymeric matrices. These include ultrasonication as well as magnetic and electrical irradiation.[21] Sonication presents an interesting option as it has been shown to improve delivery of compounds having both lipophilic and hydrophilic properties.[22–25] The possibility of using ultrasound for improved PAH transport in polymer-liquid systems has been examined by Isaza and Daugulis[16] and results showed significant enhancements in substrate delivery and degradation. Although previous results and conclusions[26–29] suggest that sonication enhances internal and external delivery, as well as partitioning coefficients, results to date for PAHs[16] cannot be adequately interpreted to identify specific effects in two-phase systems. A mass transport analysis is, therefore, required to provide such insight.

The objective of the present study was to examine the transport of PAHs from a polymer to a surrounding liquid phase (methanol) in the presence and absence of ultrasonication. To quantify the influence of ultrasonication on mass transport, a mathematical model was developed accounting for the inter- and intra-phase mass transfers and the interfacial chemical equilibrium of PAHs between the polymer and liquid phase. The model equation was solved numerically, and the unknown transport and thermodynamic parameters were obtained by minimization of least squares differences between model calculations and experimental data. Finally, predictive knowledge in solid–liquid partitioning systems was expanded using collected transport and thermodynamic properties.

Model Development

Thermo-physical processes considered

The model developed considered two separate phases—a polymer phase and a surrounding liquid methanol phase. Methanol was the chosen solvent based on its increased solubility for the target PAHs relative to aqueous media. Initially, PAHs were considered to be present in spherical polymer beads. Upon addition of the beads to methanol, transport of PAHs from the polymeric phase to the methanol phase occurred until chemical equilibrium was established. The transport of PAHs within the polymer was described by diffusion while transport into the bulk liquid phase, considered to be well-mixed, was described in terms of classical interfacial mass transfer coefficients. PAH concentrations in the bulk liquid phase were considered to change with time and were obtained from a PAH mass balance. Concentrations of PAHs in the polymer phase varied both spatially and temporally and the pertinent partial differential equation subject to appropriate initial and boundary conditions was solved.

Model assumptions

The following assumptions were made during model development:

1. Fickian diffusion appropriately described transport within the polymer (dilute solution assumption). This was a reasonable approximation since the system temperature at which transport occurred, was higher than the polymer glass transition temperature and thereby the rates of polymer chain relaxation could be assumed to be much faster than permeant movement, allowing for delivery to progress in a Fickian manner.[30]
2. The sole mechanism of transport within the polymer matrix was diffusion.
3. The system considered had constant thermophysical properties. That is, the diffusivity was independent of concentration, direction (isotropic), and presence of other PAH species.
4. Spatial distribution of PAHs was symmetric and initially uniform across the polymer.
5. Partitioning of PAHs between the polymer and methanol phases could be described by Henry's Law-type relationships. Dilute conditions allowed solid–liquid equilibria to maintain constant proportionalities.
6. There was negligible change in polymer volume due to PAH transport or polymer-solvent interactions. The polarity differences between methanol (relatively polar) and the polyurethane matrix (hydrophobic) discouraged solvent penetration and thus volume changes. The assumption was validated from manufacturer data, which demonstrated negligible polymer swelling, in methanol, after 6 months of immersion.
7. The rate of PAH partitioning was faster than Fickian transport and assumed to be spontaneous under the conditions examined.[31]
8. Constant temperature was maintained throughout the transport process.
9. Polymers pellets were approximately spherical and PAH transport was unidirectional (i.e., radial).

Mass transport equation and boundary conditions

The mathematical equation governing Fickian transport in the polymer phase was given by the following equation in one-dimensional spherical coordinates:

$$\frac{1}{D}\frac{\partial C}{\partial t} = \frac{\partial^2 C}{\partial r^2} + \frac{2}{r}\frac{\partial C}{\partial r} \tag{1}$$

where, C was the permeant concentration in the polymer phase, and D was the diffusive coefficient of the permeant in the polymer matrix.

The initial condition for polymer phase concentration was given by:

$$\text{At } t = 0; \quad C(r,\ 0) = C_o \tag{2}$$

Boundary conditions are described below via Eqs. 3 and 4. A symmetry boundary condition (Eq. 3) was applied at the centre of the spherical beads. At the polymer bead surface, the mass flux out of the polymer sphere was coupled to the mass flux into the liquid phase (Eq. 4). The liquid phase flux was described by the product of the liquid mass transfer coefficient and the difference in PAH concentrations at the polymer-liquid interface and in the well-mixed, bulk liquid phase.

$$\text{At } r = 0; \quad \frac{\partial C(0,t)}{\partial r} = 0 \tag{3}$$

$$\text{At } r = r_p; \quad -D\frac{\partial C(r_p,t)}{\partial r} = k_l(C_l - C_b) \tag{4}$$

where, C_o was the initial concentration of solutes of interest in the polymer matrix, k_l was the convective mass transfer coefficient in the solvent (adjacent to the polymer surface, where the polymer radius is r_p), C_l was the concentration in the solvent at equilibrium with that at the polymer surface, and C_b was the solute concentration in the bulk liquid phase. By definition $K_{s/l} = C_l/C_s$, where $K_{s/l}$ described the partitioning or equilibrium behavior of solutes at the polymer-liquid interface and C_s was the concentration of solute at the polymer surface.

Liquid phase concentration

Liquid concentrations were determined from the following material balance.

$$C_b(t) = \frac{\left[V_p C_o - \left(\int_0^{V_p} C(t)\cdot dV\right)\right] n_p}{V_l} \tag{5}$$

where V_p was the volume of a single polymer pellet, n_p the number of polymer bead pellets present in the liquid phase, V_l the volume of liquid, and C_b the concentration in the solvent.

Internal and external mass transfer control

The model consisted of three unknown parameters—polymer phase diffusivity (D), polymer-liquid partitioning coefficient ($K_{s/l}$), and liquid-phase convective mass transfer coefficient (k_l). Depending on the material properties and operating conditions, the rate of PAH release may be either dominated by internal mass transport (i.e., low D) or external mass transfer (k_l), or a combination of the two. The external mass transfer coefficient can be manipulated by various methods, including mixing of the liquid phase, e.g., by use of a magnetic mixer. Thus, with increasing mixing, and thereby increasing k_l, the net rate of PAH release from the polymer phase will become increasingly dominated by the internal mass transport resistance. If the external mass transport becomes sufficiently high, the internal mass transport will be the rate controlling step in the overall PAH release. It is important to indicate that for such a situation, an exact value of the k_l is not required in the mathematical model to capture the temporal behavior of the system/process. Experimentally, the condition of internal mass transfer control could be determined by increasing the mixing characteristics (e.g., rpm) until no changes in the temporal release profiles are observed with further increases in mixing speed.

In the present study, the model was applied for the condition of internal mass transport control, which was experimentally verified by confirming the similarity in the PAH release profile at two high mixing speeds.

Table 1. Polymer Properties (Obtained Through Measurements and/or Manufacturer Information)

Approximate radius per bead, r_p, (cm)	0.181
Number of polymer beads, n_p	140
Desmopan 9370A density (g/L)	1060

Solution method

The partial differential equation (PDE) subject to initial (Eq. 2) and boundary conditions (Eqs. 3 and 4) must be solved to obtain the solution. It must be noted that Crank[32] has provided an analytical solution for similar systems wherein the surrounding fluid is of finite volume (thus, solute concentrations change with time) resulting in time-varying flux and/or concentration at the spherical surface. However, the solution to the equation requires determination of non-zero roots of a non-linear equation, i.e., an iterative solution is required.

In this study, the PDE was discretized both in time and space using an implicit finite difference scheme. A linear algebraic equation for each discretized point was obtained. Thus, for a given time step, a set of linear algebraic equations representing the system of PDE for each discrete point in the computation domain was obtained. The solution to this set of equations was obtained by matrix inversion using MATLAB®.

For the computation, the model domain was divided into 100 grid points. Doubling the number of grid points resulted in less than 0.2% change in the solution. Although the implicit method was inherently stable, a time step of 1 min ensured accuracy of results (measured via regression) while reducing computational requirements.

Parameters for numerical solution

The model parameters—diffusivities (D) and partitioning coefficients ($K_{s/l}$)—were estimated using the built in MATLAB® least squares regression function, lsqcurvefit. This algorithm used an interior-reflective Newton method to determine function parameters, which best fit a series of data. Iterations involved the approximate solution to large linear systems using the method of preconditioned conjugate gradients (PCG), as described in MATLAB®. Additional polymer properties used in model developed can be found in Table 1.

Materials and Methods

Materials

Spectrophotometric grade methanol (95+%) was purchased from Fisher Scientific (Guelph, Canada).

Phenanthrene (98+%) and fluoranthene (98%) were purchased from Alfa Aesar (Ward Hill, MA) whereas pyrene (95%) and benzo[a]pyrene (BaP, 99+%, scintillation grade) were purchased from Sigma-Aldrich (Oakville, Canada). Desmopan 9370A (polyurethane elastomer beads) was graciously donated by Bayer Material Science (Leverkusen, Germany).

Analytical procedures

Analytical methods were adapted from those described by Isaza and Daugulis.[16] PAH concentrations in methanol were quantified via fluorescence spectroscopy using a QuantaMaster QM- 2000-6 fluorescence spectrometer (Photon Technology International, London, Canada). Samples were held in quartz cuvettes, type 3H, with a path length of 10 mm, obtained from NSG Precision Cells (Farmingdale, NY). Synchronous scans were performed to generate unique peaks for each PAH and the Felix32 software package was used to collect the data from the device. The detection conditions for the synchronous scan of each PAH [change in wavelength ($\Delta\lambda$), peak maximum, integration area] were, in nanometers: Phenanthrene [53.0, 346.0, 343–351], pyrene [37.0, 371.5, 369–375], fluoranthene [175.5, 460.0, 459–468], and benzo[a]pyrene [108.0, 404.0, 398–415]. All samples were diluted in methanol to within the linear range of detection (0–0.1 mg/L).[15]

PAH loading in polymer beads

Fifteen grams of Desmopan beads were equilibrated with a stock methanol solution containing all PAHs, for 24 h at 20°C, to achieve loadings of ~1.6, 1.6, 1.8, and 1 mg/g of phenanthrene, fluoranthene, pyrene, and benzo[a]pyrene, respectively. Uptake of PAHs was determined through a mass balance as detailed by Isaza and Daugulis.[16] After uptake, methanol was decanted, and polymer beads were washed with water for 3 min and allowed to air dry for 24 h to volatilize residual solvent.[15] Loaded polymer beads were then divided equally into 5 (i.e., 3 g of polymer each) vials and stored in the dark until further use.

PAH release tests

Four different release conditions were examined to address the nature of PAH transport. 15 mL of fresh methanol were introduced into the scintillation vials containing the loaded polymers, and concentrations were monitored as a function of time. At most, ~400 min were required to reach equilibrium under all conditions, and duplicate samples were obtained to address variability. Release conditions examined were natural convection (no external mixing control), 800 and 1000 rpm mixing, and sonication without additional mixing. Release tests were all carried out at 20°C and mixed conditions were achieved as detailed below.

Stirred release conditions were achieved using a Fisher Scientific Thermolyne Cimarec 3 stir plate. A Fisher Scientific ultrasonic bath (model FS20) with an output frequency and intensity of 42 kHz and 70 W (nominal intensity) was used for sonication experiments. Ultrasonic bath volumes were maintained constant in all sonication experiments by introducing equal amounts of water. The sample vial (containing the loaded polymer beads and methanol) was placed in the bath and continuous sonication was triggered while PAH concentrations, in methanol, were monitored with time. Temperature was maintained at 20°C via a recirculation loop detailed by Isaza and Daugulis.[16] Note that sample locations in the bath were maintained utilizing a clamp and retort stand, which prevented movement.

PAH partitioning coefficients from Desmopan 9370A and Methanol

Partitioning coefficient procedures were equivalent to those described by Isaza and Daugulis.[16] Equilibrium concentrations of PAHs in methanol were determined via spectrophotometry and polymer uptakes were calculated via a mass balance. Partitioning coefficients and confidence intervals, for each PAH, were determined through a least squares regression.

Results and Discussion

Release of PAHs from Desmopan 9370A into Methanol

The concentration of phenanthrene, fluoranthene, pyrene, and benzo[a]pyrene in the liquid phase (methanol) as a function of time is presented in Figure 1 under the different mixing conditions examined. Each plot represents the release profiles of the individual PAHs. It must be recalled that the four data sets for each PAH correspond to three sets in the absence of sonication—no mixing, mixing at 800 rpm, and mixing at 1000 rpm—and one set in the presence of sonication but without any additional or external mixing. The model predictions for the cases of external mixing and sonication are also presented as line plots.

Several noteworthy features can be observed in Figure 1. In all tests, an equilibrium-like condition was achieved at longer times. It must also be noted that the release rate was rapid at early times, when the driving force was large, and nearly 80% of the equilibrium concentration was attained in ~50 min. It can also be observed that the release rates for 800 and 1000 rpm mixing conditions were similar and can be considered to be the same. Additionally, for each system (PAH) examined, the three non-sonicated experiments resulted in the same final liquid phase concentration, which provided further confidence that a true equilibrium condition had been attained. One of the most interesting features of the plots was that the equilibrium concentration levels observed under sonication conditions, for all PAHs examined, was higher than those found under non-sonicated conditions.

PAH release under non-sonicated conditions

As discussed earlier, the PAH release rate for the no mixing (natural convection) condition, displayed for all PAHs in Figure 1, was slower than that found under any mixed condition, suggesting that delivery was at least partially externally controlled (at the polymer-methanol boundary layer). This is not surprising as PAHs are hydrophobic aromatics and transport into methanol, the more polar phase relative to Desmopan, would likely be restricted at the polymer-solvent boundary. Also, since the release profiles for 800 rpm and 1000 rpm tests were essentially the same, it could be concluded that under mixing conditions greater than 800 rpm, the

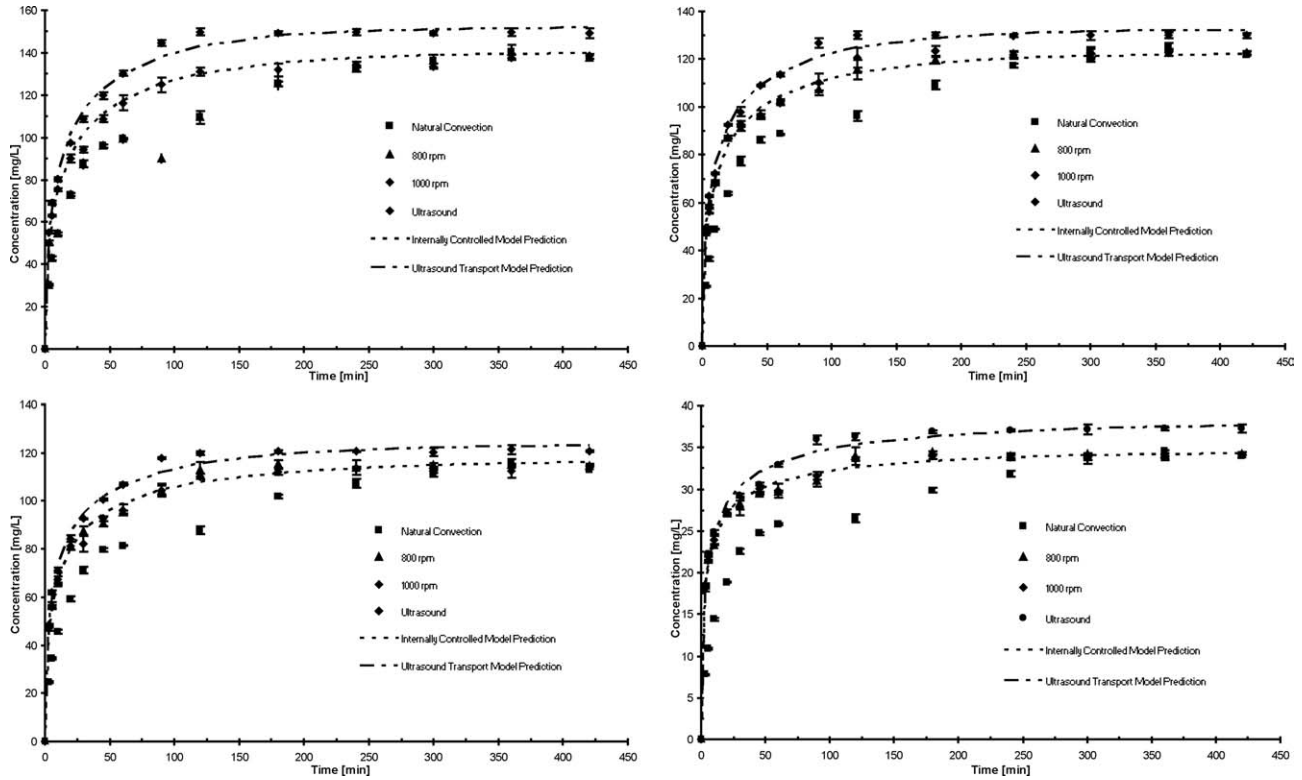

Figure 1. Release data of phenanthrene (Top Left), fluoranthene (Top Right), pyrene (Bottom Left), and benzo[a]pyrene (Bottom Right) under non-sonicated (natural convection, 800 and 1000 rpm) and sonicated conditions: dashed lines represent data obtained for non-sonicated and sonicated model predictions of all PAHs.

transport of PAHs was controlled by the internal mass transport resistance. Thus, such experimental data could be fitted without a need for estimating convective mass transfer coefficients, k_l. As an aside, it could be hypothesized that delivery of PAHs into more polar solvents, such as aqueous media, would also be externally restricted. Therefore, if sonication could yield internally controlled deliveries, significant improvements could result. Such a possibility elucidates a potential reason for the enhancements demonstrated by Isaza and Daugulis.[16]

Influence of sonication on PAH release rate and equilibrium

Data presented in Figure 1 also show that the rates of release under sonication, for all PAHs, are at least as great as those obtained for internally controlled conditions (>800 rpm). Therefore, ultrasonic irradiation appeared to remove the external mass transfer resistance. The role of sonication can be understood by recognizing that it produces "microjets,"[26] which generate turbulence at the polymer surface and in turn, reduce external resistances to the point where internal mass transport completely dominates PAH release into the surrounding liquid phase. A closer look at Figure 1 also shows that rates of release under ultrasonic exposure, for phenanthrene, fluoranthene, and pyrene were slightly faster than those obtained under internally controlled conditions, thus hinting at the possibility of improved diffusive properties. Enhancements of this nature (i.e., beyond internally controlled deliveries) would only arise from changes in internal properties and could be attributed to sonic shockwaves generating microscopic turbulence within polymer pores.[27] Similar results have been observed for delivery of various drugs from a number of polymers, in which transport increased as a function of agitation to a certain point, after which rates became independent of mixing.[29] However, as also seen in this study sonicated deliveries were faster than those observed under any mixing conditions examined, suggesting that sonic improvements were not solely external.[29]

Sonication effects on PAH transport were also found to be a function of structural and chemical solute properties. On the basis of trends displayed in Figure 1, enhancements in transport via sonication decreased with increasing PAH molecular weight/volume (Table 2). This was evident as the presence of sonication induced a more apparent enhancement in the rate of phenanthrene delivery followed by fluoranthene, pyrene, and BaP. Transport in polymers requires energy for exchange in positions between solutes and polymer chains.[30] Therefore, higher energy requirements for delivery of larger solutes, such as BaP, would lead to slower position exchanges and more restricted transport. Furthermore, BaP being the most hydrophobic PAH, likely had the strongest interactions with Desmopan resulting in reduced internal movement. Finally, based also on hydrophobicity, BaP was likely subject to the most restrictive external resistance due to its delivery into more polar methanol.

Table 2. Transport and Thermodynamic Properties Estimated in the Absence and Presence of Sonication

	Non-Sonicated	Sonicated	Percent Change*(%)
Phenanthrene (Molecular weight = 178.24 g/mol)			
Diffusion coefficient, D, (cm^2/s, $\times 10^{-7}$)	4.115 ± 0.521	5.012 ± 0.674	21.8
Partitioning coefficient, $K_{s/p}$ (unitless)	0.134 ± 0.005	0.153 ± 0.006	14.0
Fluoranthene (Molecular weight = 202.26 g/mol)			
Diffusion coefficient, D, (cm^2/s, $\times 10^{-7}$)	3.747 ± 0.347	4.502 ± 0.563	20.2
Partitioning coefficient, $K_{s/p}$ (unitless)	0.105 ± 0.002	0.117 ± 0.004	11.4
Pyrene (Molecular weight = 202.26 g/mol)			
Diffusion coefficient, D, (cm^2/s, $\times 10^{-7}$)	2.912 ± 0.400	3.471 ± 0.464	19.2
Partitioning coefficient, $K_{s/p}$ (unitless)	0.081 ± 0.002	0.087 ± 0.003	7.4
BaP (Molecular weight = 252.32 g/mol)			
Diffusion coefficient, D, (cm^2/s, $\times 10^{-7}$)	1.979 ± 0.338	1.722 ± 0.306	−14.9
Partitioning coefficient, $K_{s/p}$ (unitless)	0.036 ± 0.001	0.040 ± 0.001	11.1

Note that 95% confidence regions are provided for all parameter estimates.
*Percentage change calculated for sonicated case with respect to non-sonicated case.

Figure 1 also established that all non-sonicated release conditions (natural convection, 800 and 1000 rpm) reached the same equilibrium position as dictated by thermodynamics. However, it is apparent that sonication induced higher PAH concentrations in methanol at equilibrium with similar effects reported in previous studies.[26–28] During sonication, bubbles are generated and subsequently collapse, in a process termed cavitation, inducing conditions of several thousand Kelvin and a few hundred bar. Near a solid surface, such as a polymeric matrix, asymmetric bubble collapse forms ''microjets'' reaching speeds up to 500 m/s, which along with sonic shockwaves can break up of interactions between sorbed molecules and sorbent surfaces.[27] This condition leads to increased desorption and higher solute concentrations in the solvent, providing one plausible explanation for the phenomenon seen in Figure 1. Additionally, ultrasonic waves diffusing through particles or polymers increase the energy of sorbed molecules at balance sites causing them to vibrate more violently and desorb,[27] thus providing an additional explanation for the increased endpoint concentrations observed in Figure 1.

Quantification of diffusive and equilibrium properties for sonicated and non-sonicated systems

The diffusivity and partitioning coefficients of all PAHs were estimated for internally controlled conditions for systems not subjected to sonication (i.e., mixing >800 rpm). Experimental data collected under ultrasonic irradiation were also fitted assuming internally controlled conditions. Table 2 summarizes diffusive and thermodynamic parameters of best fit (determined through the minimization of least squares detailed in the Materials and Methods).

By examining Table 2, it is evident that for the non-sonicated case, diffusion coefficients decreased as a function of PAH molecular size. Such a trend agrees with previous notions that consider the movement within a polymer matrix to be more restricted for solutes of increased volume. Diffusivities decreased from smaller sized phenanthrene, followed by fluoranthene and pyrene, and finally BaP. It is useful to note that fluoranthene and pyrene have equivalent molecular weight and, accordingly, reduction in coefficients is further affected by more subtle property differences. However, it is clear that a trend was present between diffusivities and penetrant sizes. Similar correlations have been shown in a variety of polymers for similar aromatic compounds (benzene, toluene, p-xylene, and mesitylene) with diffusivities ranging in the order of 10^{-7} cm^2/s,[30] which validated the range of parameters estimated in the current study. Additional information by Kumar et al.[33] also supported the trend of decreased diffusivity as a function of solute size, with findings showing decreasing coefficients for benzene, toluene, and xylene, respectively, in poly(ethylene-*co*-vinyl acetate) (EVA) matrices, ranging in the order of 10^{-7} cm^2/s.[33] In another study, benzene diffusivities in various polyurethane membranes were reported to range between 10^{-5} and 10^{-7} cm^2/s,[34] comparable to the order of magnitude of diffusivities presented in Table 2. It can be hypothesized that correlations between internal transport restrictions and permeant molecular sizes are for the most part matrix independent. Such a pattern agrees with free volume theory (FVT).[33]

As outlined in FVT, the mobility of polymer segments and diffusion coefficients of permeants are a function of the polymer matrix free volume.[34] Therefore, larger molecular size solutes require higher free volumes for efficient transport. Conversely, in the case of a matrix with an established free volume, the larger the solute the more restricted its pathway and thus lower diffusion coefficient. Diffusivities determined under the presence of sonication also decreased as a function of penetrant molecular size. It appears that even in the presence of sonication, providing increased energetics, transport of larger solutes was more restricted due to free volume requirements.

From Table 2, it is also evident that partitioning coefficients obtained under sonication were significantly larger than those in the absence of irradiation. Increasing coefficients represented augmented desorption or higher concentrations of PAHs in methanol at equilibrium (also seen in Figure 1). Sonically induced shifts of this nature (towards increased desorption) have been observed for a number of solute-polymer combinations.[26–28] With the exception of BaP, the percent increase in partitioning coefficient shifts induced via sonication decreased as a function of PAH hydrophobicity (displayed in Table 2). This was not surprising as interactions between non-polar Desmopan (polyurethane) and PAHs, likely increased as a function of permeant hydrophobicity. Since the sonic energy provided was constant, the magnitude or extent of breakage of interactions

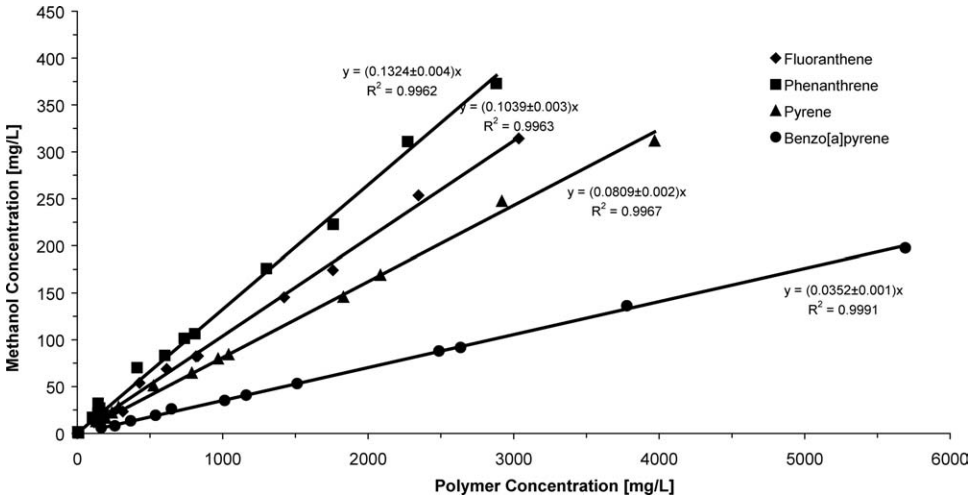

Figure 2. Experimentally determined partitioning coefficients in Desmopan 9370A and methanol of all PAHs.

decreased as function of attraction strength, which for the most part followed hydrophobic solute behaviors.

Direct determination of partitioning coefficient data from batch experiments

Independent equilibrium experiments were conducted without sonication to directly determine partition coefficients. The slope of a plot of equilibrium concentration in the liquid phase vs. corresponding equilibrium concentration in the polymer phase yielded the partitioning coefficients shown in Figure 2. By comparing parameters estimated by the fit of the model (Table 2) with those presented in Figure 2, it is evident that the partition coefficients lie within each others' 95% confidence regions. As reported in a previous study, the partition coefficients decreased as a function of PAH hydrophobicity.[15] This trend was clearly observed in Figure 2, as most lipophilic BaP, had the highest concentration in the polymer at equilibrium, relative to methanol. Pyrene, fluoranthene, and phenanthrene followed, respectively, with decreasing hydrophobicity and increasing methanol concentrations (representing higher partitioning coefficients). As an important aside, all partitioning coefficients estimated under sonicated delivery (Table 2) were also conclusively outside confidence regions presented in Figure 2, providing further evidence that ultrasonic exposure truly shifted equilibrium positions.

Correlating diffusion coefficients and partitioning coefficients to permeant structural/chemical properties

It is intuitive, and has been previously discussed in some detail, that both transport and thermodynamic parameters are a function of permeant structural and chemical properties. Polymer characteristics may also play a role, however, in this study only a single type of matrix was examined (Desmopan). Previous research indicated that partitioning coefficients of PAHs in a Desmopan-aqueous system correlated well with solute hydrophobicity, measured through octanol-water partitioning coefficients.[15] For the most part, such a trend was correct in which pyrene (log $K_{O/W} = 5.18$[35]) and fluoranthene (log $K_{O/W} = 5.20$[36]), having higher octanol-water coefficients than phenanthrene (log $K_{O/W} = 4.46$[37]), correlated well with polymer-aqueous thermodynamic parameters.[15] A similar assessment could be made for the coefficients determined in this study. However, the relationship presented could not be extended to explain the behavior of pyrene and fluoranthene whose polymer-methanol partitioning coefficients differed, but log $K_{O/W}$ values were approximately equivalent. This demonstrated a limitation in the ability of log $K_{O/W}$ to predict PAH partitioning coefficients in polymer-methanol systems. Figure 3 demonstrates such a correlation for both partitioning and diffusive coefficients.

It is evident from Figure 3 that the overall trend presented for log $K_{O/W}$ also correlated well with transport parameters. Since log $K_{O/W}$ is typically proportional to increasing PAH molecular sizes,[38] it is not surprising that the diffusion coefficient trend, discussed previously, could be extended to log $K_{O/W}$. Though an overall trend is clear, there is an apparent discontinuity in Figure 3 where log $K_{O/W}$ fails to describe differences in thermodynamic and transport behaviors of pyrene and fluoranthene, which have equivalent molecular weights. This may be due to log $K_{O/W}$'s inability to account for certain chemical and/or attractive effects between penetrants and polymer-methanol environments. Recognizing the

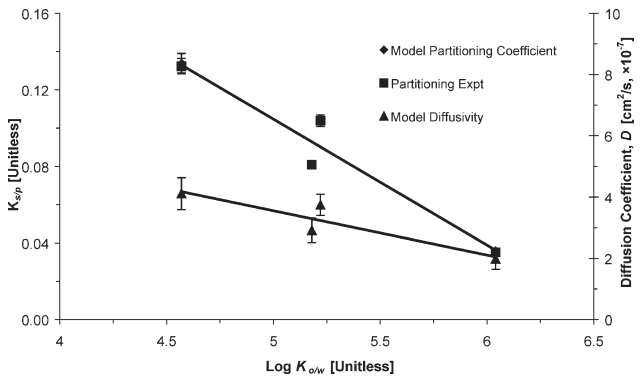

Figure 3. Transport and thermodynamic parameters as a function of PAH octanol-water partitioning coefficients.

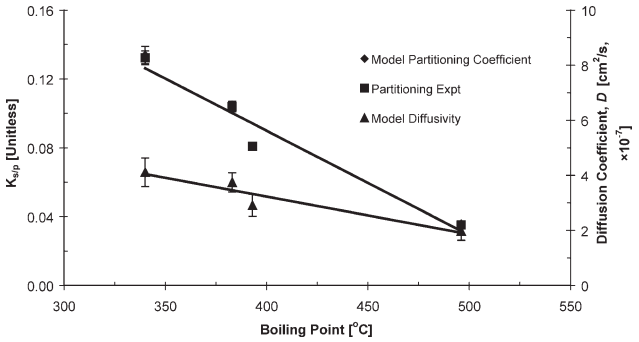

Figure 4. Transport and thermodynamic parameters correlated as a function of PAH Boiling Point.

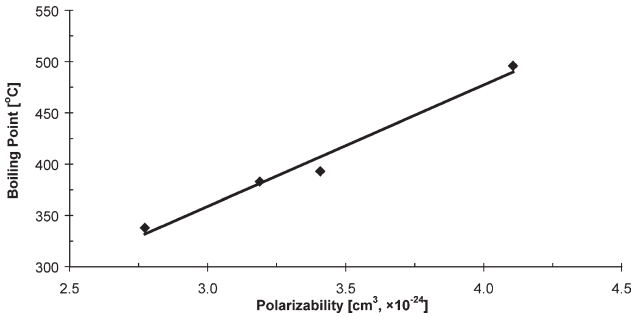

Figure 6. Boiling Point of PAHs as a function of polarizability (converted to SI units from reported atomic units).

aforementioned deficiency, boiling point (BP) was chosen as a secondary descriptor.

BP is another material property capturing structural and chemical permeant characteristics of a species, which correlates with thermodynamic and transport parameters. The diffusion coefficient and partitioning coefficients were plotted as a function of the BP of the PAHs and the results are presented in Figure 4. From the figure, it is evident that diffusivities and partitioning coefficients estimated correlated well with BPs (phenanthrene—340°C,[38] fluoranthene—383°C,[38] pyrene—393°C,[38] and benzo[a]pyrene—496°C).[38] However, BP does not provide an indication as to the independent properties that induce such an accurate correlation. Differences in BP arise from structural and chemical properties and need to be dissected as such to provide further insight.

Statistical studies have examined a series of thermodynamic, electronic, steric, and topological descriptors of PAHs to develop quantitative structure-property relationships (QSPR) with BPs, log $K_{O/W}$ and others.[38] Figure 5 demonstrates the correlation between BP and molecular volume (MV)[38] of PAHs examined in this study, which displayed the same inconsistency discussed for log $K_{O/W}$. This was due to the fact that MV is strictly a structural property incapable of accounting for chemical and/or attractive effects. The same outcome was observed for the correlation of BP and molecular weight (MW). As a final measure, a correlation between BP and Randic index was examined as discussed in a previous study.[38] The Randic connectivity index measures the sum of relative accessibility areas in the molecule.[39] This area represents the total area accessible for molecular

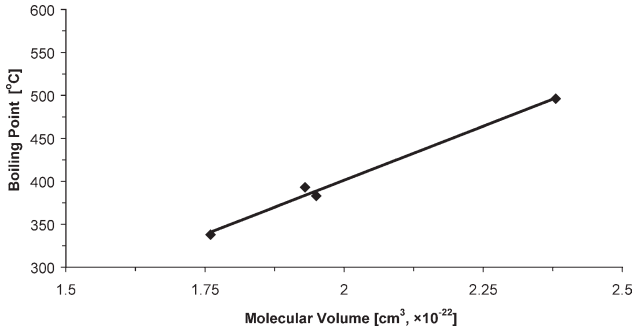

Figure 5. Boiling Point of PAHs as a function of PAH molecular volume.

interactions with surroundings. However, based on such a definition, it is evident that the Randic index is again a structural property and, therefore, unable to fully account for chemical/attractive interactions.

A closer examination revealed that polarizability (an additional descriptor reported by Alves de Lima Ribeiro and Ferreira[38]) provided an accurate correlation for BP. Figure 6 displays such a relationship. It is likely that polarizability is one of the properties captured by BP, which allowed for its excellent description of transport and thermodynamic parameters of the PAHs examined. Plotting diffusivities and partitioning coefficients, in the absence of sonication, as a function of polarizability yielded the results shown in Figure 7. Note that the accuracy of the results was as expected since the linear correlation between BP and polarizability, seen in Figure 6, implied an efficient description of diffusion/partition coefficients.

Polarizability indicates the ease with which a species can be deformed by an electric field.[38] Additionally, one of the most polarizing influences on a particular species is the presence of another species in the nearby surroundings. Therefore, it provides a measure of attraction between PAHs and their polymer-methanol environment. As discussed in previous studies,[40] interactions of PAHs and polymeric matrices arise from Van der Waals attractions. The magnitude of this attraction is dictated by the instantaneous and induced dipole moments, which depend on the polarizability of the molecule. Therefore, as polarizability increases via increased size and/or molecular arrangement, so do Van der Waals attractions, thus explaining the patterns observed for PAHs which were more efficiently sorbed onto Desmopan by virtue of their increased Van der Waals attraction for the polymeric surface. In terms of partitioning coefficient differences between fluoranthene and pyrene, it seems that polarizability captures attractive interactions. Pyrene being more polarizable, relative to fluoranthene, has a stronger attraction for the more hydrophobic polymer resulting in its lower partitioning coefficient. As for transport properties, pyrene and fluoranthene diffusivities vary as a function of polarizability demonstrating that attractive interactions play a role in delivery. It can be suggested that stronger pyrene-polymer attractions significantly delayed its movement through the matrix and resulted in decreased diffusivities, relative to fluoranthene. Overall, it appears that polarizability adequately correlates linearly with transport and thermodynamic properties

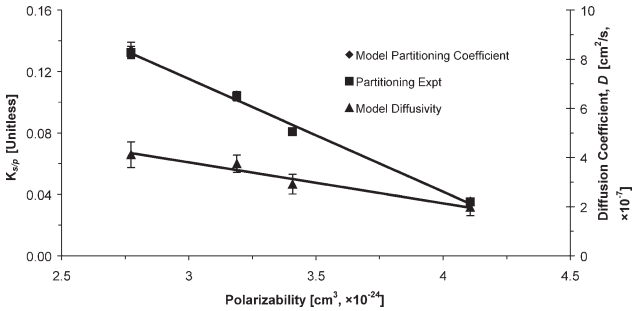

Figure 7. Transport and thermodynamic parameters correlated as a function of polarizability: note that polarizability was converted to SI units from reported atomic units.

accounting for both molecular size and chemical/attractive properties. As a final note, future work will attempt to validate the model, while also deconstructing and including the polarizability trend discussed. Such an addition would provide a deeper fundamental understanding of transport and thermodynamic behaviors of PAHs in solid–liquid systems.

Conclusions

In the current study, it was determined that the transport of PAHs from Desmopan into methanol was influenced by external mass transport resistance in the solvent phase. Enhanced mixing conditions yielded faster release rates of PAHs to an extent, after which the overall transport was limited entirely by internal resistances at mixing speeds of 800 rpm or greater. Release rates for phenanthrene, fluoranthene, and pyrene in the presence of sonication were also slightly faster than those found under any mixing conditions examined, suggesting possible improvements in polymer transport properties. Additionally, the presence of ultrasonic exposure conclusively shifted thermodynamic positions inducing higher concentrations of PAHs in solution at equilibrium. Such an observation is well in accordance with current sonochemistry knowledge. Furthermore, the model developed was capable of describing the transport of all PAHs in the presence and absence of sonication, as well as quantifying both diffusive and thermodynamic properties. The diffusivities of phenanthrene, fluoranthene, pyrene, and BaP, with or without sonication decreased as a function of molecular size and were in the order of 10^{-7} cm^2/s. These were in agreement with coefficients of similar aromatic compounds in a variety of polymer matrices. In addition, partitioning coefficients estimated with and without sonication conclusively differed from each other and a trend of decreased coefficients, and thus affinity for Desmopan, as a function of molecular size was demonstrated. Finally, thermodynamic and transport parameters were correlated with a series of permeant properties yielding factors usable for predictive purposes in polymer-solvent systems. Polarizability was the most accurate descriptor found in the current study.

Literature Cited

1. Juhasz AL, Naidu R. Bioremediation of high molecular weight polycyclic aromatic hydrocarbons: a review of the microbial degradation of benzo[a]pyrene. *Int Biodeterior Biodegrad*. 2000;45:57–88.
2. Cerniglia CE. Fungal metabolism of polycyclic aromatic hydrocarbons: past, present and future applications in bioremediation. *J Ind Microbiol Biotechnol*. 1997;19:324–333.
3. Cerniglia CE. Biodegradation of polycyclic aromatic hydrocarbons. *Biodegradation*. 1992;3:351–368.
4. Denys S, Rollin C, Guillot F, Baroudi H. In situ phytoremediation of PAHs contaminated soils following a bioremediation treatment. *Water Air Soil Pollut: Focus*. 2006;6:299–315.
5. Onwudili JA, Williams PT. Flameless supercritical water incineration of polycyclic aromatic hydrocarbons. *Int J Energy Res*. 2006;30:523–533.
6. Antizar-Ladislao B, Lopez-Real J, Beck AJ. Degradation of polycyclic aromatic hydrocarbons (PAHs) in an aged coal tar contaminated soil under in-vessel composting conditions. *Environ Pollut*. 2006;141:459–468.
7. Kulik N, Goi A, Trapido M, Tuhkanen T. Degradation of polycyclic aromatic hydrocarbons by combined chemical pre-oxidation and bioremediation in creosote contaminated soil. *J Environ Manage*. 2006; 78:382–391.
8. Birman I, Alexander M. Optimizing biodegradation of phenanthrene dissolved in nonaqueous-phase liquids. *Appl Microbiol Biotechnol*. 1996;45:267–272.
9. Bouchez M, Blanchet D, Vandecasteele JP. Substrate availability in phenanthrene biodegradation: transfer mechanism and influence on metabolism. *Appl Microbiol Biotechnol*. 1995;43:952–960.
10. Muñoz R, Guieysse B, Mattiasson B. Phenanthrene biodegradation by an algal-bacterial consortium in two-phase partitioning bioreactors. *Appl Microbiol Biotechnol*. 2003;61:261–267.
11. Vandermeer KD, Daugulis AJ. Enhanced degradation of a mixture of polycyclic aromatic hydrocarbons by a defined microbial consortium in a two-phase partitioning bioreactor. *Biodegradation*. 2007;18:211–221.
12. Daugulis AJ, McCracken CM. Microbial degradation of high and low molecular weight polyaromatic hydrocarbons in a two-phase partitioning bioreactor by two strains of Sphingomonas sp. *Biotechnol Lett*. 2003;25:1441–1444.
13. Janikowski TB, Velicogna D, Punt M, Daugulis AJ. Use of a two-phase partitioning bioreactor for degrading polycyclic aromatic hydrocarbons by a Sphingomonas sp. *Appl Microbiol Biotechnol*. 2002;59:368–376.
14. Villemur R, Déziel E, Benachenhou A, Marcoux J, Gauthier E, Lepine F, Beaudet R, Cameau Y. Two-liquid-phase slurry bioreactors to enhance the degradation of high-molecular-weight polycyclic aromatic hydrocarbons in soil. *Biotechnol Prog*. 2000;16:966–972.
15. Rehmann L, Prpich GP, Daugulis AJ. Remediation of PAH contaminated soils: application of a solid–liquid two-phase partitioning bioreactor. *Chemosphere*. 2008;73:798–804.
16. Isaza PA, Daugulis AJ. Ultrasonically enhanced delivery and degradation of PAHs in a polymer-liquid partitioning system by a microbial consortium. *Biotechnol Bioeng*. 2009;104:91–101.
17. Daugulis AJ. Two-phase partitioning bioreactors: a new technology platform for destroying xenobiotics. *Trends Biotechnol*. 2001;19: 457–462.
18. Amsden BG, Bochanysz J, Daugulis AJ. Degradation of xenobiotics in a partitioning bioreactor in which the partitioning phase is a polymer. *Biotechnol Bioeng*. 2003;84:399–405.
19. Déziel E, Comeau Y, Villemur R. Two-liquid-phase bioreactors for enhanced degradation of hydrophobic/toxic compounds. *Biodegradation*. 1999;10:219–233.
20. Rehmann L, Daugulis AJ. Biodegradation of biphenyl in a solid–liquid two-phase partitioning bioreactor. *Biochem Eng J*. 2007;36:195–201.
21. Kost J, Langer R. Responsive polymeric delivery systems. *Adv Drug Deliv Rev*. 2001;46:125–148.
22. Kost J, Leong K, Langer R. Ultrasonically controlled polymeric drug delivery. *Makromol Chem Macromol Symp*. 1988;19:275–285.
23. Levy D, Kost J, Meshulam Y, Langer R. Effect of ultrasound on transdermal drug delivery to rats and guinea pigs. *J Clin Invest*. 1989;83:2074–2078.
24. Miyazaki S, Hou WM, Takada M. Controlled drug release by ultrasound irradiation. *Chem Pharm Bull*. 1985;33:428–431.
25. Miyazaki S, Yokouchi C, Takada M. External control of drug release: controlled release of insulin from a hydrophilic polymer

implant by ultrasound irradiation in diabetic rats. *J Pharm Pharmacol*. 1988;40:716–717.
26. Breitbach M, Bathen D. Influence of ultrasound on adsorption processes. *Ultrasonics-Sonochemistry*. 2001;8:277–283.
27. Ji J, Lu X, Xu Z. Effect of ultrasound on adsorption of Geniposide on polymeric resin. *Ultrasonics-Sonochemistry*. 2006;13:463–470.
28. Li Z, Li X, Xi H, Hua B. Effects of ultrasound on adsorption equilibrium of phenol on polymeric adsorption resin. *Chem Eng J*. 2002;86:375–379.
29. Kost J, Leong K, Langer R. Ultrasound-enhanced polymer degradation and release of incorporated substances. *Proc Natl Acad Sci USA*. 1989;86:7663–7666.
30. Harogoppad SB, Aminabhavi TM. Interactions of substituted benzenes with elastomers. *Polymer*. 1991;32:870–876.
31. Cesário MT, Beverloo WA, Tramper J, Beeftink HH. Enhancement of gas-liquid mass transfer rate of apolar pollutants in the biological waste gas treatment by a dispersed organic solvent. *Enzyme Microb Technol*. 1997;21:578–588.
32. Crank J. *The Mathematics of Diffusion*. Oxford: Oxford University Press, 1979.
33. Kumar SA, Thomas S, Kumaran MG. Transport of aromatic hydrocarbons through poly(ethylene-*co*-vinyl acetate) membranes. *Polymer*. 1997;38:4629–4640.
34. Ponangi R, Pintauro PN, De Kee D. Free volume analysis of organic vapor diffusion in polyurethane membranes. *J Membr Sci*. 2000;178:151–164.
35. Means JC, Wood SG, Hassett JJ, Banwart WL. Sorption of polynuclear aromatic hydrocarbons by sediments and soils. *Environ Sci Technol*. 1980;14:1524–1528.
36. Scheele B. Reference chemicals as aids in evaluating a research program-selection aims and criteria. *Chemosphere*. 1980;9:293–309.
37. Hansch C, Fujita T. p-σ-π Analysis. A method for the correlation of biological activity and chemical structure. *J Am Chem Soc*. 1964;86:1616–1626.
38. Alves de Lima Ribeiro F, Ferreira MMC. QSPR models of BP, octanol-water partition coefficient and retention time index of polycyclic aromatic hydrocarbons. *J Mol Struct (Theochem)*. 2003;663:109–126.
39. Estrada E. The structural interpretation of the randic index. *Internet Electron J Mol Des*. 2002;1:360–366.
40. Valderrama C, Gamisans X, de las Heras FX, Cortina JL, Farrán A. Kinetics of polycyclic aromatic hydrocarbons removal using hypercross-linked polymeric sorbents Macronet Hypersol MN200. *React Funct Polym*. 2007;67:1515–1529.

Manuscript received May 29, 2009, revision received Sept. 10, 2009, and final revision received Dec. 15, 2009.